ERDC/CHL CR-15-1

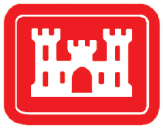

US Army Corps
of Engineers®
Engineer Research and
Development Center

ERDC
INNOVATIVE SOLUTIONS
for a safer, better world

Three-Dimensional Shallow Water Adaptive Hydraulics (ADH-SW3): Turbulence Closure

Gaurav Savant

June 2015

Coastal and Hydraulics Laboratory

The US Army Engineer Research and Development Center (ERDC) solves the nation's toughest engineering and environmental challenges. ERDC develops innovative solutions in civil and military engineering, geospatial sciences, water resources, and environmental sciences for the Army, the Department of Defense, civilian agencies, and our nation's public good. Find out more at www.erdc.usace.army.mil.

To search for other technical reports published by ERDC, visit the ERDC online library at http://acwc.sdp.sirsi.net/client/default.

ERDC/CHL CR-15-1
June 2015

Three-Dimensional Shallow Water Adaptive Hydraulics (ADH-SW3): Turbulence Closure

Gaurav Savant

Dynamic Solutions LLC
6421 Deane Hill Dr. Suite 1.
Knoxville, TN 37919

Final report

Prepared for U.S. Army Corps of Engineers
Washington, DC 20314-1000

Monitored by Coastal and Hydraulics Laboratory
U.S. Army Engineer Research and Development Center
3909 Halls Ferry Road, Vicksburg, MS 39180-6199

Abstract

The U.S. Army Engineer Research and Development Center (ERDC), Coastal and Hydraulics Laboratory (CHL), has undertaken the development of the multimodule Adaptive Hydraulics (ADH) hydrodynamic, sediment, water quality, and transport numerical code. The Mellor-Yamada level 2.5 and k-ε turbulence closure models were incorporated into ADH-SW3. This report documents the incorporation of these turbulence closure models into ADH-SW3; it also documents the validation of their incorporation by using them in an application of the ADH-SW3 model code to three flume experiments. These flume tests were designed to ensure that the incorporated turbulence closure models in ADH-SW3 are solving the pertinent equations accurately. A basic description of other turbulence closure options implemented with ADH-SW3 is also provided, and a user manual (User Appendix) is included.

Contents

Figures and Tables

Figures

Tables

Preface

This report presents the details of incorporating the Mellor-Yamada level 2.5 and k-ε turbulence closure schemes into the three-dimensional shallow water module of the Adaptive Hydraulics (ADH-SW3) numerical code. The report also briefly describes other turbulence models incorporated into ADH-SW3 and includes a user manual (User Appendix). This investigation was conducted from October 2013 through March 2014 at the U.S. Army Engineer Research and Development Center (ERDC) by Dr. Gaurav Savant of Dynamic Solutions LLC.

This report is published as a product of the Flood and Coastal Storm Damage Reduction Program of the ERDC, Vicksburg, MS. Dr. Cary Talbot was the Program Manager, and William Curtis was the Technical Director.

At the time of publication of this report, Dr. Jeffery P. Holland was Director of ERDC, and LTC John T. Tucker III was Acting Commander.

Unit Conversion Factors

Multiply	By	To Obtain
cubic feet	0.02831685	cubic meters
cubic yards	0.7645549	cubic meters
degrees (angle)	0.01745329	radians
feet	0.3048	meters
knots	0.5144444	meters per second
microns	1.0 E-06	meters
miles (nautical)	1,852	meters
miles (U.S. statute)	1,609.347	meters
miles per hour	0.44704	meters per second
pounds (force)	4.448222	newtons
slugs	14.59390	kilograms
square feet	0.09290304	square meters
square miles	2.589998 E+06	square meters
square yards	0.8361274	square meters
yards	0.9144	meters

1 Introduction

The U.S. Army Corps of Engineers (USACE), through the U.S. Army Engineer Research and Development Center (ERDC), has developed a robust multidimensional mass conservative finite element hydrodynamic and constituent transport numerical code Adaptive Hydraulics (ADH). Adaptive Hydraulics has been referred to as "ADH" and "AdH" in literature; the abbreviation ADH is used in this report in accordance with how Adaptive Hydraulics is referenced in peer-reviewed literature.

The objectives of this study were to incorporate the Mellor-Yamada level 2.5 (MY-25) and k-ε turbulence closure schemes into ADH-SW3, document the incorporation and the verification and validation of the schemes, and provide a user manual (User Appendix). Both MY-2.5 and k-ε models involve the solution of two transport equations to represent the generation and dissipation of turbulent energy. These two models have the capability to represent several real-world phenomena such as density stratification and adverse pressure flow. Additionally, other closures exist in the ADH-SW3 code — the Mellor-Yamada level 2 and the Smagorinsky — and a brief description of those is presented for comparison and completeness. Validation of these closures was documented in Savant et al. (2014).

2 Equation Development

Basic equations

A variety of three-dimensional (3D) reservoir, riverine, coastal, and estuarine simulation models (e.g., ADH-SW3, CH3D, TABS-MDS) exist. These models solve some form of the Reynolds-averaged Navier-Stokes equations using the hydrostatic assumption. The governing equations for velocity $U_i = (U,V,W)$, and constituent C in $x_i = (x,y,z)$ is written as

$$\frac{\partial U_j}{\partial x_j} = 0 \tag{1}$$

$$\frac{\partial U_i}{\partial t} + \frac{\partial (U_i U_j)}{\partial x_j} - \frac{1}{\rho_0}\frac{\partial P}{\partial x_i} - \frac{1}{\rho_0}\left(\frac{\partial}{\partial z} K_m \frac{\partial}{\partial z} U_i\right) - F_i = 0 \tag{2}$$

where j is summed over (x, y, z) or (U, V, W) and i is (x, y) or (U, V), as appropriate; the equation for the z-direction component reduces to

$$P(z) = P_a + \int_z^{\eta} g\rho(z)dz \tag{3}$$

under the hydrostatic pressure assumption, where P_a is the atmospheric pressure, g is the acceleration due to gravity, $\rho(z)$ is the density at a location in the z-direction, and η is the water surface elevation.

In addition, the convection-diffusion equation for a baroclinic transport constituent is written as

$$\frac{\partial C}{\partial t} + \frac{\partial}{\partial x_j}(U_j C) - \frac{\partial}{\partial z} K_h \frac{\partial C}{\partial z} + F_C = 0 \tag{4}$$

with the sum over j as before.

Coefficients for the horizontal viscosity (F_i) and horizontal diffusivity (F_C) terms are generally calculated using a horizontal closure scheme,

Smagorinsky for ADH-SW3. The vertical eddy viscosity for momentum ($K_m \equiv E_{xz} = E_{yz}$) and eddy diffusivity for transport ($K_h \equiv D_z$) coefficients are utilized to represent the Reynolds stresses and turbulence transport. Estimates of these coefficients are obtained by turbulence closure schemes, which are discussed in the following sections.

Horizontal eddy viscosity and diffusivity – Smagorinsky

Coefficients for the horizontal eddy viscosity $\left(F_i\right)$ and horizontal diffusivity (F_C) terms are generally calculated using a horizontal closure scheme.

These terms are usually represented as

$$F_i = \frac{1}{\rho_0}\left(\frac{\partial}{\partial x_j} E_{ij} \frac{\partial U_i}{\partial x_j}\right) \tag{5}$$

$$F_C = \frac{\partial}{\partial x_j} D_j \frac{\partial C}{\partial x_j} \tag{6}$$

where j is summed over (x, y) or (U, V) and i is (x, y), as appropriate. ADH-SW3 applies the Smagorinsky (1963) technique to calculate the coefficients E_{xx}, E_{xy}, E_{yy}, E_{yx}, D_x, and D_y. The formulation takes the form

$$E_{xx} = E_{yy} = E_{xy} = D_x = D_y = c_s \Delta \sqrt{\left[\left(\frac{\partial U}{\partial x}\right)^2 + \left(\frac{\partial V}{\partial x}\right)^2 + \left(\frac{\partial U}{\partial y}\right)^2 + \left(\frac{\partial V}{\partial y}\right)^2 + 2\left(\frac{\partial U}{\partial y}\frac{\partial V}{\partial x} - \frac{\partial U}{\partial x}\frac{\partial V}{\partial y}\right)\right]} \tag{7}$$

where c_s is the Smagorinsky coefficient ($0.05 < c_s < 0.1$) and Δ is the element area.

Generic length scale (GLS) implementation

To facilitate the incorporation of additional turbulence closure schemes, MY-2.5 and k-ε in ADH-SW3 were implemented using the GLS scheme proposed by Umlauf and Burchard (2003). The GLS scheme is a two-equation turbulence model that takes advantage of the similarities between most two-equation models. The first equation represents the transport and evolution of the standard turbulent energy (k), and the second equation represents the transport and evolution of a generic

quantity (ψ). A generic quantity (ψ) is used to establish the turbulence length scale (l). The equation for k is represented as

$$\frac{\partial k}{\partial t}+U_j\frac{\partial k}{\partial x_j}-\frac{\partial}{\partial z}\left(\frac{K_m}{\sigma_k}\frac{\partial k}{\partial z}\right)-(P+B-\varepsilon)=0 \tag{8}$$

where j is summed over (x, y, z) or (U, V, W), as appropriate, σ_k is the turbulence Schmidt number for k (Table 1), P and B represent the generation of turbulence by shear and buoyancy production or destruction by density gradients, respectively, and ε is the dissipation of turbulence. P, B and ε are represented as

$$P=K_m M^2 \tag{9}$$

with

$$M^2=\left(\frac{\partial U}{\partial z}\right)^2+\left(\frac{\partial V}{\partial z}\right)^2 \tag{10}$$

$$B=-K_h N^2 \quad , \quad N^2=-\frac{g}{\rho_0}\frac{\partial \rho}{\partial z} \tag{11}$$

$$\varepsilon=\left(c_\mu^0\right)^{3+\frac{p}{n}}k^{\frac{3}{2}+\frac{m}{n}}\psi^{\frac{-1}{n}} \tag{12}$$

where ρ_0 is the density at standard temperature and pressure (STP), c_μ^0 is a model stability coefficient, and m, n, and p are model specific parameters (Table 1).

The second equation describes the evolution and transport of a generic parameter (ψ), and is specified as

$$\frac{\partial \psi}{\partial t}+U_j\frac{\partial \psi}{\partial x_j}-\frac{\partial}{\partial z}\left(\frac{K_m}{\sigma_\psi}\frac{\partial \psi}{\partial z}\right)-\frac{\psi}{k}\left(c_1 P+c_3 B-c_2 \varepsilon F_{wall}\right)=0 \tag{13}$$

where j is summed over (x, y, z) or (U, V, W), as appropriate, c_1, c_2 and c_3 are model specific parameters (Table 1), σ_ψ is the turbulence Schmidt number for ψ (Table 1), and

$$\psi = \left(c_{\mu}^{0}\right)^{p} k^{m} l^{n} \tag{14}$$

The turbulent length scale (l) is recovered through

$$l = \left(c_{\mu}^{0}\right)^{3} k^{\frac{3}{2}} \varepsilon^{-1} \tag{15}$$

The MY-2.5 model requires the specification of a wall function (F_{wall}), several formulations of which are presented in the literature. Details of the wall function are provided later in this report.

Careful selection of parameters p, m, n, F_{wall}, c_1, c_2, c_3, σ_k, and σ_ψ results in the recovery of exact formulations for the MY-2.5 and k-ε turbulence closure schemes.

Table 1. GLS Parameters

	k-kl	k-ε
p	0.0	3.0
m	1.0	1.5
n	1.0	-1.0
σ_k	2.44	1.0
σ_ψ	2.44	1.3
c_1	0.9	1.44
c_2	0.5	1.92
c_3	0.9	1.0
c_μ^0	0.5544	0.5544

Mellor-Yamada level 2.5 (MY-2.5) GLS implementation

The MY-25 scheme is reproduced from (8) and (13) using the k-kl column in Table 1 and specifying p = 0.0, m = 1.0 and n = 1.0, yielding

$$\frac{\partial k}{\partial t} + U_j \frac{\partial k}{\partial x_j} - \frac{\partial}{\partial z}\left(K_Q \frac{\partial k}{\partial z}\right) - (P + B - \varepsilon) = 0 \tag{16}$$

and

$$\frac{\partial kl}{\partial t}+U_j\frac{\partial kl}{\partial x_j}-\frac{\partial}{\partial z}\left(K_Q\frac{\partial kl}{\partial z}\right)-\frac{\psi}{k}\left(c_1P+c_3B-c_2\varepsilon F_{wall}\right)=0 \tag{17}$$

The original implementation of MY-2.5 defined K_Q as

$$K_Q=lS_q\sqrt{2k} \tag{18}$$

where S_q = 0.2.

In the GLS implementation of MY-25, K_Q is defined as

$$K_Q=\frac{K_m}{\sigma_q} \tag{19}$$

where σ_q is the Schmidt number for k and takes a value of 2.44, $\sigma_k=\sigma_\psi$, c_1 = 0.9, c_2 = 0.5, and c_3 = 0.9.

The wall function can be prescribed as originally suggested in Mellor-Yamada (1982)

$$F_{wall}=2h-d_b \tag{20}$$

or as

$$F_{wall}=\left(1+E_2\left(\frac{l}{\kappa}\frac{1}{MIN\left(d_s,d_b\right)}\right)^2\right) \tag{21}$$

as suggested by Burchard et al. (1998) or as

$$F_{wall}=\left(1+E_2\left(\frac{l}{\kappa}\frac{1}{d_s}\right)^2\right) \tag{22}$$

as suggested by Burchard (2001) for deep basins, or as the following which was suggested by Blumberg et al. (1992) for general open channel flows

$$F_{wall} = \left(1 + E_2\left(\frac{l}{\kappa d_b}\right)^2 + E_4\left(\frac{l}{\kappa d_s}\right)^2\right) \tag{23}$$

In the ADH-SW3 implementation, each of the wall functions is implemented, where E_2 = 1.33, E_4 = 0.25, κ is the von Karman constant and takes a value of 0.4, h is the flow depth, d_s is distance to surface, and d_b is distance to the bed. Experience has shown that Equation (23) is the wall function that is likely most useful for estuaries, and Equation (21) is more appropriate to riverine applications.

The vertical eddy viscosity for momentum (K_m) and eddy diffusivity for transport (K_h) coefficients are obtained by appealing to formulations involving stability functions. These are represented as

$$K_m = S_m l\sqrt{2k} \tag{24}$$

$$K_h = S_h l\sqrt{2k} \tag{25}$$

where S_m and S_h are stability functions for momentum and transport, respectively, and are derived algebraically (Warner et al. 2005).

There are several formulations of S_m and S_h available, such as Kantha and Clayson (1994), Galperin et al. (1988), and Canuto et al. (2001) among several others, in the literature. The ADH-SW3 implementation of MY-25 uses the formulation described by Kantha and Clayson (1994) and is described as

$$S_h = \frac{A_2\left(1 - \frac{6A_1}{B_1}\right)}{1 - 3A_2G_h\left[6A_1 + B_2\left(1 - C_3\right)\right]} \tag{26}$$

$$S_m = A_1\left\{\frac{\left(1 - \frac{6A_1}{B_1} - 3C_1\right) + 9\left[2A_1 + A_2\left(1 - C_2\right)\right]S_hG_h}{\left(1 - 9A_1A_2G_h\right)}\right\} \tag{27}$$

with

$$G_h = \frac{(l)^2}{k} N^2 \quad , \quad -0.28 \le G_h \le 0.0233 \tag{28}$$

Kantha and Clayson (1994) stability function parameter values are presented in Table 2.

Table 2. MY-25 stabilization function parameters.

Parameter	A_1	A_2	B_1	B_2	C_1	C_2	C_3	G_h, min	G_h, max
Value	0.92	0.74	16.6	10.1	0.08	0.7	0.2	-0.28	0.0233

The GLS formulation imposes an upper limit on the length scale (l) to account for the reduction in mixing in stable stratification. Warner et al. (2005) present this limit as

$$l^2 \le \frac{0.56l}{N^2} \quad , \quad N^2 > 0 \tag{29}$$

Vertical eddy viscosity through Mellor-Yamada level 2 (MY-2)

ADH-SW3 has the option of computing the coefficients K_m and K_h using the MY-2 scheme described in Mellor and Yamada (1982). This closure scheme is a simplification of the MY-2.5 scheme: it neglects diffusion, equates the generation of turbulent energy with its dissipation, and assumes horizontal homogeneity. In essence, it is a turbulence equilibrium model (i.e., any turbulence generated or transported is instantaneously dissipated). This implies that

$$P + B = \varepsilon \tag{30}$$

Equation (30) and Mellor and Yamada's (1982) assumption that turbulent energy is destroyed as it is created, and thus not transported, in essence removes Equations 16 and 17 from the computation. (For a detailed discussion of the MY-2 scheme, see Mellor and Yamada (1982)).

MY-2 does not follow the assumptions in the GLS scheme, and to obtain the MY-2 formulation, the basic equations developed by Mellor and Yamada (1982) must be used. These equations include defining the length scale (l) as

$$l = \kappa d_b \tag{31}$$

or as

$$l = \kappa d_b \left[1 - \frac{d_b}{h}\right] \tag{32}$$

where all variables are as previously defined. Equation 31 (Mellor and Blumberg 2004) is widely used and provides a linear shape for the mixing length. ADH-SW3 uses equation 32 similar to that suggested by Robert and Ouellet (1987). In the absence of surface waves, Equation 32 goes to 0 at the surface and at the bed. If the master length scale is assumed to be specified as above or by some other relationship, a flux Richardson number (R_f) is defined as

$$R_f = -\frac{S_h N^2}{S_m M^2} \tag{33}$$

The gradient Richardson number (R) is defined as

$$R = -\frac{N^2}{M^2} \tag{34}$$

or

$$R = \frac{S_m}{S_h} R_f \tag{35}$$

Mellor-Yamada (1982) defined the following as the energy budget for the turbulent kinetic energy:

$$S_m \frac{l^2}{k} M^2 + S_h \frac{l^2}{k} N^2 = B_1^{-1} \tag{36}$$

This can be further written as

$$1 - R_f = \frac{1}{\left(\frac{l^2}{k}\right) B_1 S_m M^2} \tag{37}$$

Utilizing the above and definitions for M^2 and N^2, the turbulent momentum and constituent transport coefficients are written as

$$K_m = S_m l^2 \left|\frac{\partial u}{\partial z}\right| \left[S_m B_1 \left(1 - R_f\right)\right]^{0.5} \tag{38}$$

and

$$K_h = S_h l^2 \left|\frac{\partial u}{\partial z}\right| \left[S_m B_1 \left(1 - R_f\right)\right]^{0.5} \tag{39}$$

K-ε GLS implementation

The k-ε model is retrieved from the GLS model described by Equations (8) through (15) by utilizing the parameters specified in the k-ε column of Table 1. The equations for turbulent kinetic energy (k) and the dissipation (ε) are written in GLS as

$$\frac{\partial k}{\partial t} + U_j \frac{\partial k}{\partial x_j} - \frac{\partial}{\partial z}\left(\frac{K_m}{\sigma_k^{\varepsilon}} \frac{\partial k}{\partial z}\right) - (P + B - \varepsilon) = 0 \tag{40}$$

where all quantities are the same as previously described. σ_k^{ε} is the Schmidt number for eddy diffusivity of k and has a value of 1.0, and

$$\frac{\partial \varepsilon}{\partial t} + U_j \frac{\partial \varepsilon}{\partial x_j} - \frac{\partial}{\partial z}\left(\frac{K_m}{\sigma_{\varepsilon}} \frac{\partial \varepsilon}{\partial z}\right) - \frac{\varepsilon}{k}\left(c_1 P + c_3 B - c_2 \varepsilon\right) = 0 \tag{41}$$

where K_m is calculated using Equations 12, 14, 15 and 24, and $\sigma_{\varepsilon} \equiv \sigma_{\psi}$ is the eddy diffusivity for ε with a value of 1.3.

Boundary specification

Two-equation turbulence models do not resolve the viscous sublayer, so boundary conditions are applied in order for the models to accurately represent the turbulence transport processes. The boundary conditions for the MY-25 and k-ε two-equation turbulence models can be specified by assuming that production of turbulence by shear (P) is completely balanced by the dissipation of that turbulence (ε). Generation of turbulent kinetic

energy through buoyancy is negligible since density gradients tend towards zero.

The resulting boundary conditions for k are (Warner et al. 2005)

$$k_b = \frac{\left(u_b^*\right)^2}{\left(c_\mu^0\right)^2}, \qquad k_s = \frac{\left(u_s^*\right)^2}{\left(c_\mu^0\right)^2} \tag{42}$$

where k is the turbulent kinetic energy as before, c_μ^0 is the model specific constant (Table 1), u^* is the shear velocity, and the subscripts *b* and *s* represent bed and surface, respectively.

The resulting boundary conditions for ψ are (Warner et al. 2005)

$$\psi_b = \left(c_\mu^0\right)^{p-2m}\left(u_b^*\right)^{2m}\left(\kappa z_b\right)^n, \qquad \psi_s = \left(c_\mu^0\right)^{p-2m}\left(u_s^*\right)^{2m}\left(\kappa z_s\right)^n \tag{43}$$

where *p*, *m*, and *n* are model specific constants (Table 1), κ is the von Karman constant, and z_b and z_s are the mixing depths for bottom and surface, respectively. Stability concerns require that the value of z_s is specified as 0.01 (in the units of model), and z_b is specified as 1% of the depth. The shear velocities for the surface and bed are calculated using

$$u_b^* = \frac{\kappa\bar{u}}{ln\left(\frac{h}{z_0}\right) - 1 + \frac{z_0}{h}}, \text{ and } \quad u_s^* = \frac{\kappa w_w}{ln\left(\frac{h}{z_0}\right) - 1 + \frac{z_{s0}}{h}} \tag{44}$$

where $\bar{u}$ is the depth averaged flow velocity, w_w is the wind velocity, *h* is the flow depth , z_0 is the bottom roughness height, and z_{s0} is the surface roughness height and is equal to z_0 in the absence of surface waves and to 0.85 times the root mean square (RMS) wave height in the presence of surface waves (Mellor and Blumberg 2004).

Minimum values of turbulence generation and dissipation

Turbulence generation and dissipation values appear in the denominator terms for several computed quantities; this necessitates the specification of minimum values for both. Experience has shown that these minimum

values are application specific, and the user must determine the minimum values required for stability.

Buoyancy suppression functions

It is well known that stable stratification reduces momentum transfer across a pycnocline, and several formulations exist to suppress the eddy viscosity and diffusivity across this high-density gradient region. ADH-SW3 provides a choice of five functions to suppress eddy viscosity and diffusivity, each defined as a modification of K_m and K_h.

Henderson-Sellers

Henderson and Sellers (1982) derived a suppression formulation based on observations of the atmospheric boundary layer, and is represented as

$$K_m = \frac{K_m}{\left[1+0.74R\right]} \tag{45}$$

$$K_h = \frac{K_h}{\left[1+37R^2\right]} \tag{46}$$

Munk-Anderson

Munk and Anderson (1948) were some of the first researchers to observe and detail the influence of stable stratification on momentum transfer across a pycnocline based on observations of oceanic thermoclines. They provided the following modifier to the vertical eddy viscosity and diffusivity:

$$K_m = \frac{K_m}{\left[1+\beta(n_1)R\right]^{n_1}} \tag{47}$$

$$K_h = \frac{K_h}{\left[1+\beta(n_2)R\right]^{n_2}} \tag{48}$$

Values of parameters n_1, n_2, $\beta(n_1)$ and $\beta(n_2)$ are provided in Table 3.

Table 3. Buoyancy suppression function parameters.

	n_1	n_2	$\beta(n_1)$	$\beta(n_2)$	ADH-SW3 Option
Henderson-Sellers	1	1	0.74	37	1
Munk-Anderson	0.5	1.5	10	3.3	2
Kent-Pritchard	2	--	0.24	--	3
Pritchard	2	--	0.28	--	4
French-McCutcheon	2	--	10	--	5

Kent-Pritchard

Kent and Pritchard (1957) derived their suppression function from data collected in the James River Estuary and is represented as

$$K_{m,h} = \frac{K_{m,h}}{\left[1+\beta(n_1)R\right]^{n_1}} \tag{49}$$

Pritchard

Pritchard (1960) re-evaluated observations from the James River Estuary and represented his formulation as

$$K_{m,h} = \frac{K_{m,h}}{\left[1+\beta(n_1)R\right]^{n_1}} \tag{50}$$

French-McCutcheon

French and McCutcheon (1983) derived their suppression formulation from observed data in the Great Ourse Estuary, and their formulation takes the form

$$K_{m,h} = \frac{K_{m,h}}{\left[1+\beta(n_1)R\right]^{n_1}} \tag{51}$$

Note that though Equations (47) to (51) have similar forms, the values of $\beta(n)$ vary by more than an order of magnitude. Furthermore, these functions are based on empirical data, and care should be exercised in their application.

3 Testing

Testing of MY-2.5 and k-ε was performed on three test cases. The first case tested the generation/dissipation of turbulence due to high-velocity gradients in the absence of density gradients; the second case tested the generation/dissipation of turbulence primarily due to high density gradients; the third case tested the performance of the model for flow past a cylindrical obstruction in the flow path. The third test case is a particularly difficult test for any hydrostatic code because of the vertical accelerations involved; in the absence of robust turbulence models, the code will fail to simulate, in particular, the bottom currents or the downstream vortices. MY-2 and Smagorinsky closure schemes have been tested previously (Savant et al. 2014) and will not be considered.

Flow around an emergent spur dike

This test case, based upon the work presented in Rajaratnam and Nwachukwu (1983), is designed to test the accuracy and adequacy of the turbulence closure schemes implemented into ADH-SW3.

The test domain is illustrated in Figure 1. An emergent spur of 0.152 meters (m) length and 0.03 m width is placed 14.0 m downstream of the inflow location (at the left boundary). A uniform flow of 0.0453 cubic meters per second (m^3/s) is applied at the left boundary with a tail water elevation of 0.189 m applied at the right boundary.

Figure 1. Domain for spur dike test.

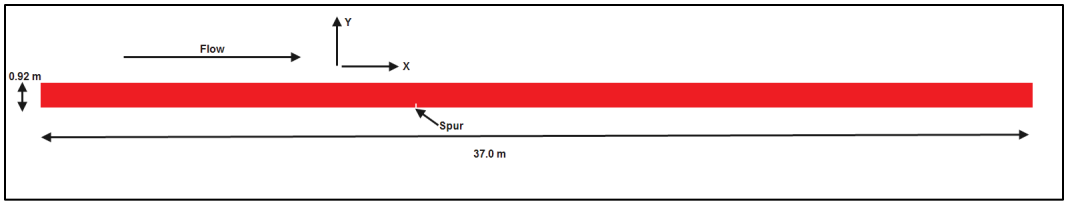

The model parameters utilized are as follows:

Smagorinsky coefficient: 0.2
Uniform background eddy viscosity: 0.0015 square meters per second (m^2/s)
Manning's *n* value: 0.01.
Minimum k: 0.000005 m^2s^{-2}

Minimum ψ or ε: 0.0005 m^2s^{-3}

Number of vertical layers: 4.

Figures 2 and 3 show the recirculation zone computed by MY-25 and k-ε, respectively. The recirculation lengths computed were 11.8 and 12.3 by MY-25 and k-ε, respectively. These values match the value of 12 times the spur length reported in literature (Wang et al. 2009).

Figure 2. Recirculation zone and velocity magnitudes with MY-25 (the color ramps from slow to fast velocity, with red representing velocities > 0.25 m/s).

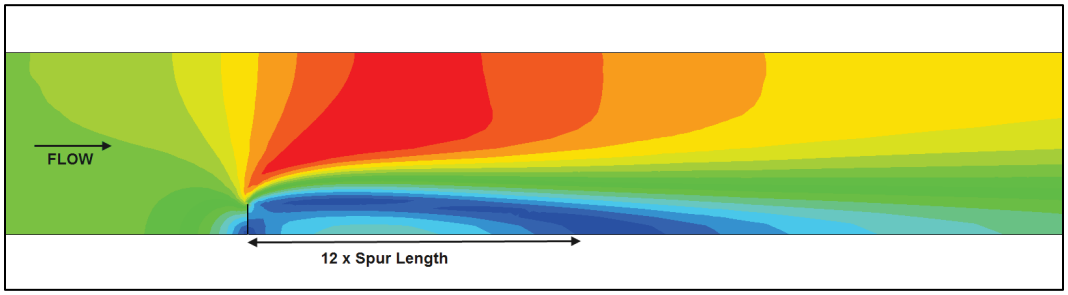

Figure 3. Recirculation zone and velocity magnitudes with k-ε (the color ramps from slow to fast velocity, with red representing velocities > 0.25 m/s).

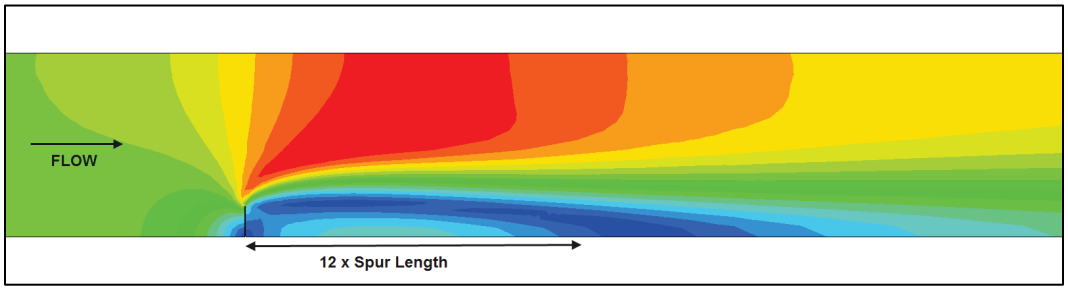

The average velocity in the domain at steady state was computed by the model to be 0.257 m/s using MY-25 and 0.282 m/s using k-ε. A close match between the two provides further confidence that both MY-25 and k-ε were implemented correctly for a high-velocity gradient case.

Propagation of salinity subsequent to a lock exchange

This test was run to ascertain the ability of the model to accurately represent the speed (U) of a density wedge, referred to as the *shock* speed in Shin et al. (2004). The test consisted of a 2 m long, 0.2 m wide, and 0.2 m deep flume with denser salt water, 35 parts per thousand (ppt), in the left half and freshwater, 0 ppt, in the right half. The barrier separating the two is instantaneously removed allowing the denser fluid to slump under the lighter fluid and move as a density wedge. As in Shin et al. (2004), U is

determined by noting the time (t) for the salinity to increase a certain amount a distance (x), from the initial separating barrier: $U = x/t$. Figures 4 and 5 illustrate the domain and initial constituent state, respectively, for this test.

Figure 4. Domain for lock exchange.

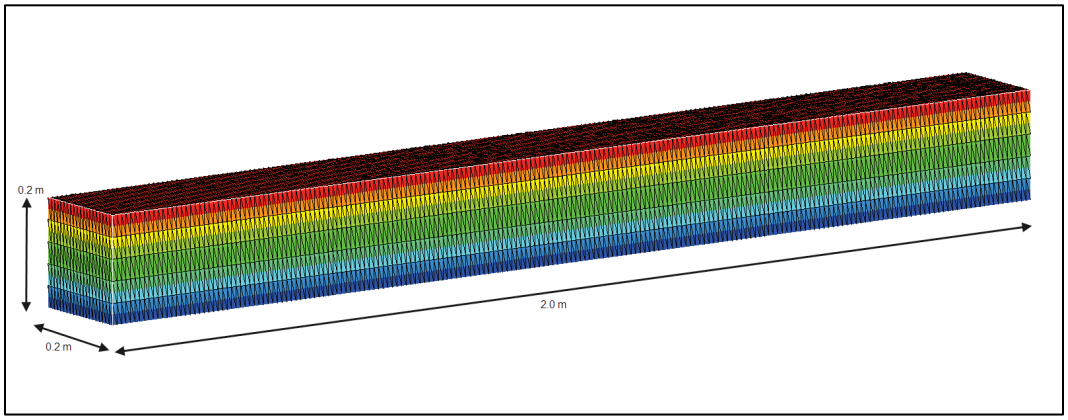

Figure 5. Initial constituent state for lock exchange.

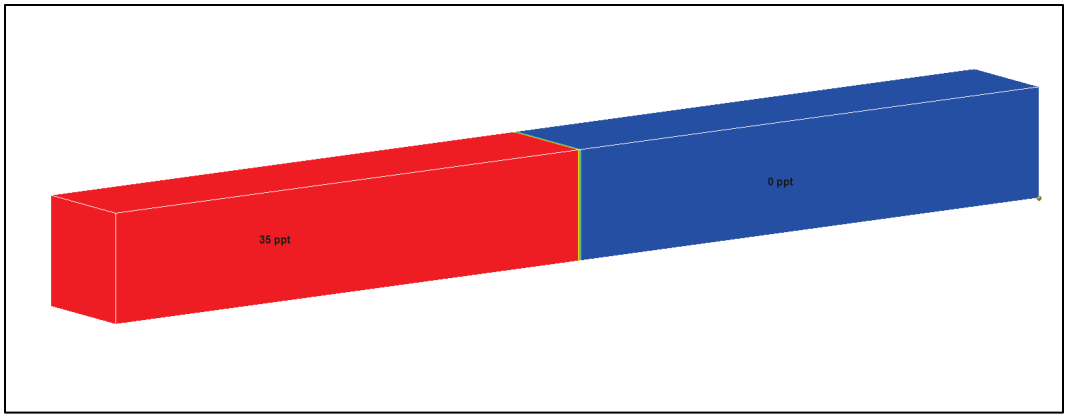

The model-computed shock speed is used to calculate the densiometric Froude number as

$$F_h = \frac{U}{\sqrt{g(1-\gamma)h}} \tag{52}$$

where γ is the ratio of lower density to higher density (0.997 for this test) and h is the total dense fluid depth. The F_h computed for this test case is 0.51 for MY-25 and 0.5 for k-ε; Shin et al. (2004) reported the value of 0.5 for the energy-conserving value of nonrigid lid density currents (Shin et al. 2004), as calculated with ADH-SW3 here.

The model parameters utilized are as follows:

Smagorinsky coefficient: 0.2
Uniform background eddy viscosity: 0.0000001 m^2/s
Manning's *n* value: 0.01
Minimum k: 0.000005 m^2s^{-2}
Minimum ψ or ε: 0.00000001 m^2s^{-3}
Buoyancy suppression function: Henderson-Sellers
Number of vertical layers: 5

Figures 6 and 7 illustrate the results, showing the position of the red salinity wedge, for the MY-25 and k-ε closure schemes tests after time 10 s. It is observed that MY-25 is slightly more diffusive compared to k-ε. The reason for this diffusivity is unclear at present and is a subject of investigation.

Figure 6. State of density wedge at 10 s with MY-25 scheme.

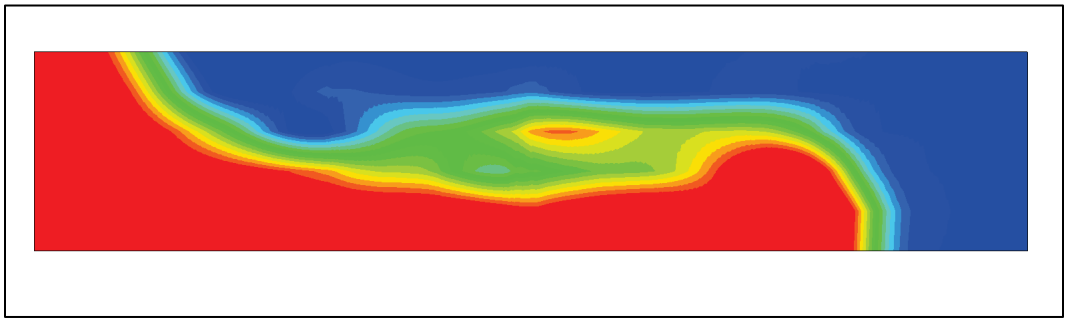

Figure 7. State of density wedge at 10 s with k-ε scheme.

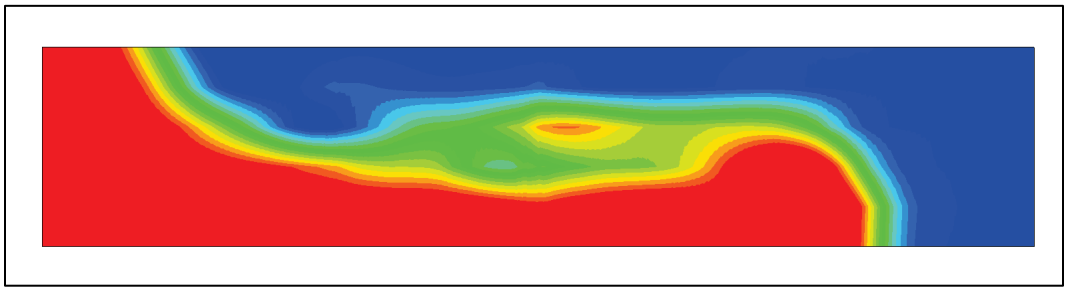

Flow around a cylindrical obstruction

This test case, roughly based upon the work of Melville and Raudkivi (1977), was designed to test the adequacy of the turbulence closure schemes to qualitatively model flow conditions where flow separation occurs and vertical accelerations are significant. ADH-SW3 is a hydrostatic code and assumes negligible vertical accelerations; hence, the burden of

accounting for these vertical accelerations rests entirely on the turbulence closure schemes implemented.

Figure 8 illustrates the domain for this test case. A solid cylinder, 5 m in diameter, is placed at a distance of 200 m from the upstream end, and flow has to go around the cylinder causing flow separation and plunging of flow. The inflow is specified as 2000 m^3/s, and a constant tail water elevation of 10 m is specified at the downstream end.

Figure 8. Domain for flow around a cylinder test.

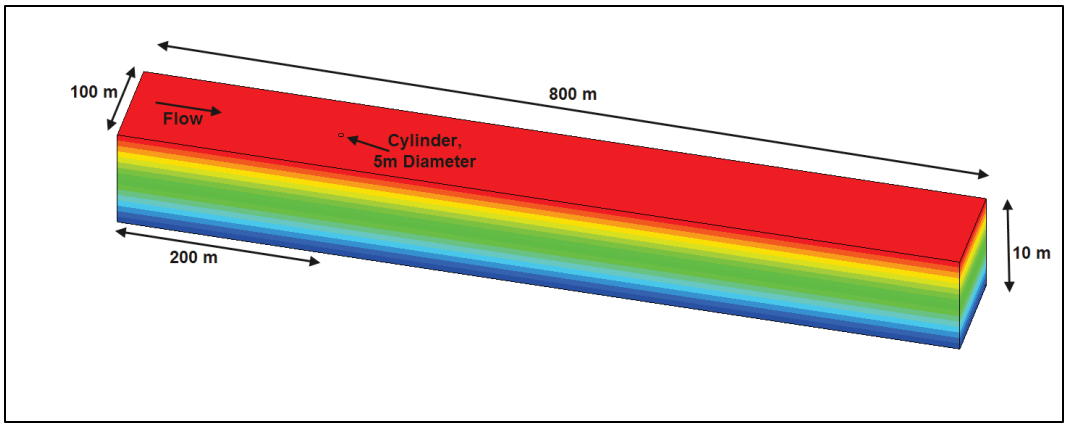

The model parameters utilized are as follows:

Smagorinsky coefficient: 0.2
Uniform background eddy viscosity: 0.0000001 m^2/s
Manning's *n* value: 0.01
Minimum k for MY-25: 0. 000001m^2s^{-2}
Minimum ψ for MY-25 or ε: 0.5 m^2s^{-3}
Minimum k for k-ε: 0. 05 m^2s^{-2}
Minimum ψ or ε for k-ε: 0.05 m^2s^{-3}
Buoyancy suppression function: Kent-Pritchard
Number of Vertical Layers: 5

Melville and Raudkivi (1977) present results from mobile bed experiments and present some velocity results from a case before initiation of bed scour. The observed results show that flow reaches stagnation upstream of the cylinder, and downstream flow separation and reattachment occurs (on the cylinder, opposite of the upstream stagnation point). Figures 9 and 10 provide the bottom streamtraces for simulated results from the MY-25 and k-ε schemes, respectively. Comparing the simulation results with those

provided by Melville and Raudkivi (1977, Figure 2, where velocity results from a case before initiation of bed scour [i.e., a flat bed] are shown), it is noted that both schemes adequately represent the bottom velocity behavior. The k-ε scheme provides a better representation of the downstream eddies, whereas the MY-25 scheme is too diffusive and results in smaller/weaker eddies. In the absence of exact experimental data, it is not possible to comment quantitatively on the performance of the two schemes.

Figure 9. Bottom streamtrace, MY-25. Red indicates higher velocity and blue lower.

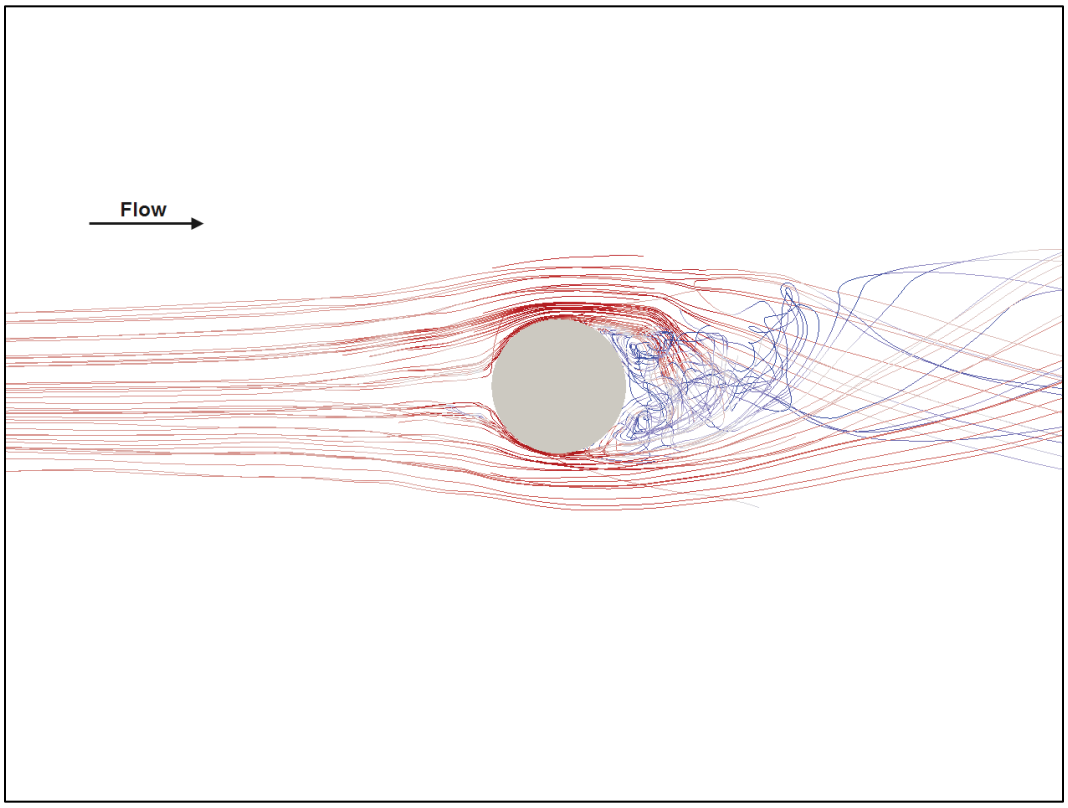

Figure 10. Bottom streamtrace, k-ε. Red indicates higher velocity and blue lower.

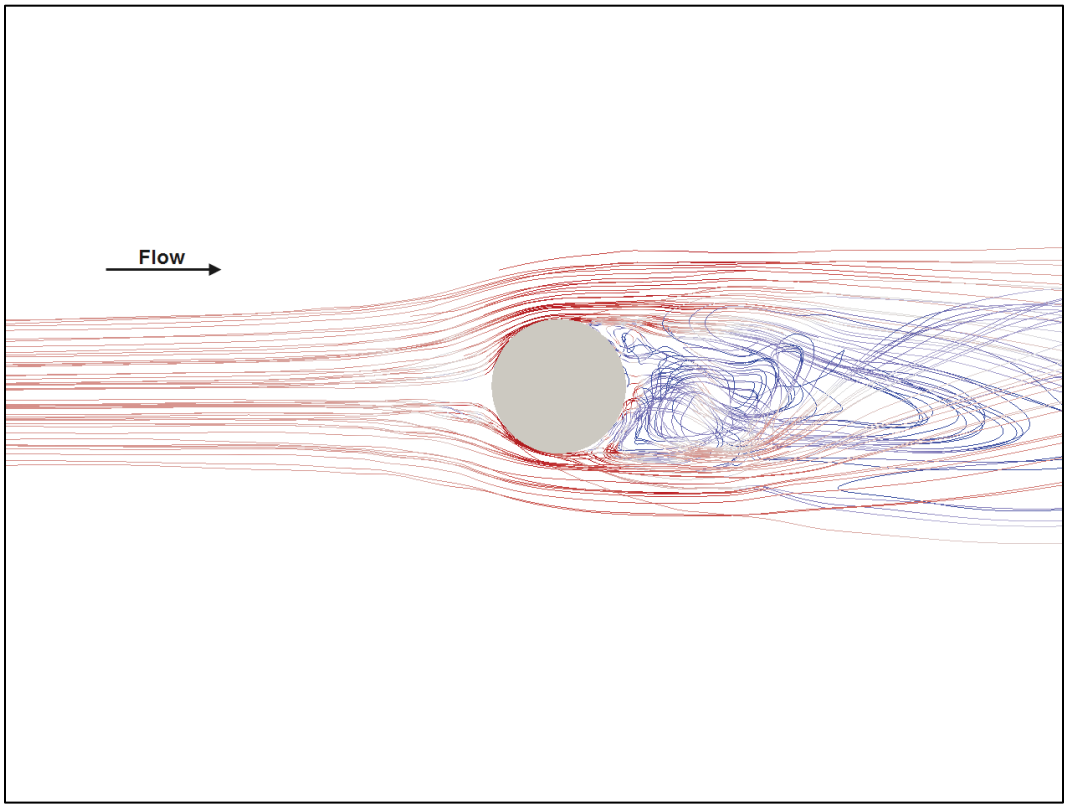

4 Summary and Conclusions

This report presents the development and incorporation of generalized length scale based Mellor-Yamada level 2.5 (MY-25) and k-ε turbulence closure schemes into the 3D shallow water module of ADH (ADH-SW3). Also presented are the details of other turbulence schemes available within ADH-SW3 (Mellor Yamada level 2 and Smagorinsky), the wall functions implemented for the MY-25 scheme, the buoyancy suppression functions available, and details of three test cases.

The three test cases were designed to exercise the turbulence closure schemes under a high-velocity gradient, under a high-density gradient, and under significant vertical accelerations. Both MY-25 and k-ε were able to accurately represent the physics of the problems. It was observed that for the high-density gradient test case, the MY-25 was slightly more diffusive than the k-ε closure scheme. The reason for this is under active investigation; the preliminary thinking is that the difference in diffusivity is due to the wall function utilized in MY-25(the (k-ε) scheme does not require a wall function).

Future work in turbulence closure is required, and it is suggested that an option be included in ADH-SW3 to write out nodal eddy viscosity and diffusivity values. The capability to write out the model-computed eddy viscosity values by node is essential to visualize model behavior; this is especially important to perform an analysis of density stratification. This is not possible at present because ADH-SW3 considers eddy viscosity and diffusivity as elemental properties.

References

Blumberg, A. F., B. Galperin, and D. J. O'Connor. 1992. Modeling vertical structure of open-channel flows. *Journal of Hydraulic Engineering* 118: 1119–1134.

Burchard, H. 2001. On the q^2l equation by Mellor and Yamada (1974). Notes and correspondence. *Journal of Physical Oceanography* 31: 1377–1387.

Burchard, H., O. Petersen, and T. Rippeth. 1998. Comparing the performance of the Mellor-Yamada and the k-e two-equation turbulence models. *Journal of Geophysical Research* 103: 10543–10554.

Canuto, V. M., A. Howard, Y. Cheng, and M. S. Dubovikov. 2001. Ocean turbulence I: One-point closure model. Momentum and heat vertical diffusivities. *Journal of Physical Oceanography* 31: 1413–1426.

French, R. H., and S. C. McCutcheon. 1983. *Turbulent vertical momentum transfer in stratified environments*. Publication No. 41079. Las Vegas, NV: Desert Research Institute.

Galperin, B., L. H. Kantha, S. Hassid, and A. Rosati. 1988. A quasi-equilibrium turbulence energy model for geophysical flows. *Journal of Atmospheric Sciences* 45: 55–62.

Henderson-Sellers, B. 1982. A simple formula for vertical eddy diffusion coefficients under conditions of non-neutral stability. *Journal of Geophysical Research* 57(C8): 5860–5864.

Kantha, L. H., and C. A. Clayson. 1994. An improved mixed layer model for geophysical applications. *Journal of Geophysical Research* 99: 25235–25266.

Kent, R. E., and D. W. Pritchard. 1957. A test of mixing length theories in a coastal plain estuary. *Journal of Marine Research* 18(1): 62–72.

Mellor, G., and A. Blumberg. 2004. Wave breaking and ocean surface layer thermal response. *Journal of the American Meteorological Society* 34: 693–698.

Mellor, G. L., and T. Yamada. 1982. Development of a turbulence closure model for geophysical fluid problems. *Reviews of Geophysics and Space Science* 20(4): 851–875.

Melville, B. W., and A. J. Raudkivi. 1977. Flow characteristics in local scour at bridge piers. *Journal of Hydraulic Research* 15(4): 373–380.

Munk, W. H., and E. R. Anderson. 1948. Notes on a theory of the thermocline. *Journal of Marine Research* 7: 276.

Pritchard, D. W. 1960. The movement and mixing of contaminants in tidal estuaries. In *Proceedings of the First International Conference on Waste Disposal in the Marine Environment*. University of California at Berkeley. New York: Pergamon Press..

Rajaratnam, N., and B. A. Nwachukwu. 1983. Flow near groin-like structures. *Journal of Hydraulic Engineering* 109(3): 463–480.

Robert, J. L., and Y. Ouellet. 1987. A *three-dimensional finite element model for the study of steady and non-steady natural flows*. Elsevier Oceanography Series, No. 45. Amsterdam, The Netherlands: Elsevier.

Savant, G., R. C. Berger, T. O. McAlpin, and C. J. Trahan. 2014. *Three dimensional shallow water adaptive hydraulics (ADH-SW3): Hydrodynamic verification and validation*. ERDC/CHL TR-14-7, Vicksburg, MS: U.S. Army Engineer Research and Development Center.

Shin, J. O., S. B. Dalziel, and P. F. Linden. 2004. Gravity currents produced by lock exchange. *Journal of Fluid Mechanics* 521: 1–34.

Smagorinsky, J. 1963. General circulation experiments with the primitive equations I. The basic experiment. *Monthly Weather Review* 91(3): 99–164.

Umlauf, L., and H. Burchard. 2003. A generic length-scale equation for geophysical turbulence models. *Journal of Marine Research* 61: 235–265.

Wang, S. S. Y., Y. Jia, P. J. Roche, P. E. Smith, and R. A. Schmalz. 2009. *Verification and validation of 3D free surface flow models*. Reston, VA: American Society of Civil Engineers.

Warner, J. C., C. R. Sherwod, H. G. Arango, and R. P. Signell. 2005. Performance of four turbulence closure models implemented using a generic length scale method. *Ocean Modeling* 8: 81–113.

Appendix: User's Guide for Turbulence Options

Turbulence cards

The turbulence options in ADH-SW3 are activated using the "MP TUR" card and the turbulence dirichlet boundaries are specified using "DB TRI" cards. Specification of boundary conditions for turbulence constituents is not mandatory but is recommended for stability purposes and consistency with published literature.

If a turbulence scheme other than Mellor-Yamada level 2 (MY-2) is used, the user must specify "CN TKE" and "CN TDS" for the turbulent kinetic energy and turbulence dissipation, respectively. The format of these cards is as follows:

CN TKE "Transport number" "Reference concentration"

CN TKE "Transport number" "Reference concentration"

Turbulence control cards

MP TUR

TURBULENCE PARAMETERS

Field	Type	Value	Description
1	char	MP	Card type
2	char	TUR	Parameter
3	int	> 0	Material number (not string)
4	int	≥ 0	Horizontal turbulence
5	int	any int	Vertical turbulence
6	real	any real	Horizontal turbulence coefficient
7	int	>0	Buoyancy suppression function

If the vertical turbulence option specified is Mellor-Yamada 2.5 or option "2", an additional card for the wall function must be specified and is

8	int	1-4	Wall proximity function

If the vertical turbulence option specified is greater than "1," additional card values must be specified and are

9	real	>0	Minimum turbulent kinetic energy (TKE)
10	real	>0	Minimum turbulent dissipation (TDS)
10	real	>0	Maximum mixing length fraction

Table A1 presents field 4, 5, 7, and 8 value options that activate various turbulence schemes as well as the buoyancy suppression functions in ADH-SW3.

Table A 1. Field parameter values.

Field 4	Field 5	Field 7	Field 8
Smagorinsky - 0	Mellor-Yamada Level 2 - 1	Henderson-Sellers - 1	Mellor-Yamada – 1
Water Surface Slope - 1	Mellor-Yamada Level 2.5 - 2	Munk-Anderson – 2	Burchard et al. – 2
	k-e - 3	Kent-Pritchard – 3	Burchard – 3
	No vertical turbulence < 0	Pritchard – 4	Blumberg et al. - 4
		French-McCutcheon - 5	

Since turbulence options are material region specific parameters, the user can specify different turbulence options and/or parameters for various material regions within the simulation.

DB TRI

TURBULENCE BOUNDARY

Field	Type	Value	Description
1	char	DB	Card type
2	char	TRI	Parameter
3	int	> 0	Node string number
4	int	> 0	Transport constituent
5	int	0 or 1	Surface or wall/bottom
6	int	any int	Vertical turbulence option

Guidance for buoyancy suppression function

The buoyancy suppression function utilized has a direct and substantial impact on the diffusion of momentum and energy across the pycnocline; this is especially true for stable stratification. The choice of which function to use is based on the type of environment being modeled.

Testing performed using ADH-SW3 has provided the following basic guidance for selection of the buoyancy suppression function:

1. Henderson-Sellers is best suited for systems that do not have stable stratification or for a relatively mixed estuarine/riverine system. Examples include estuaries such as Galveston Bay.
2. Munk-Anderson and French-McCutcheon are suited for systems that have a substantial freshwater input into a large estuary and have density stratification. Examples include estuaries such as Mobile Bay.
3. Kent-Pritchard and Pritchard are not recommended except for experimental testing due to a lack of confidence in the data utilized to develop the buoyancy suppression function.

Since turbulence options are material region specific parameters, the user can specify different turbulence options and/or parameters for various material regions within the simulation.

REPORT DOCUMENTATION PAGE

Form Approved
OMB No. 0704-0188

1. REPORT DATE	2. REPORT TYPE	3. DATES COVERED *(From - To)*
June 2015	Contract Report	*Oct 2013- March 2014*

4. TITLE AND SUBTITLE

Three Dimensional Shallow Water Adaptive Hydraulics (ADH-SW3): Turbulence Closure

5a. CONTRACT NUMBER

5b. GRANT NUMBER

5c. PROGRAM ELEMENT NUMBER

6. AUTHOR(S)

Gaurav Savant

5d. PROJECT NUMBER

5e. TASK NUMBER

5f. WORK UNIT NUMBER

7. PERFORMING ORGANIZATION NAME(S) AND ADDRESS(ES)
Engineer Research and Development Center
3909 Halls Ferry Rd
Vicksburg, MS 39180

8. PERFORMING ORGANIZATION REPORT NUMBER

ERDC/CHL CR-15-1

9. SPONSORING/MONITORING AGENCY NAME(S) AND ADDRESS(ES)
Engineer Research and Development Center
3909 Halls Ferry Rd
Vicksburg, MS 39180

10. SPONSOR/MONITOR'S ACRONYM(S)
ERDC

11. SPONSOR/MONITOR'S REPORT NUMBER(S)
N/A

12. DISTRIBUTION/AVAILABILITY STATEMENT
Approved for public release, distribution is unlimited

13. SUPPLEMENTARY NOTES

14. ABSTRACT

The U.S. Army Engineer Research and Development Center (ERDC) Coastal and Hydraulics Laboratory (CHL) has undertaken the development of the multi-module Adaptive Hydraulics (ADH) hydrodynamic, sediment, water quality and transport numerical code. The Mellor-Yamada level 2.5 and k-e turbulence closure models were incorporated into ADH-SW3. This report documents the incorporation of these turbulence closure models into ADH-SW3.

15. SUBJECT TERMS
Adaption
ADH
ADH-SW3
Finite element modeling
k-e
Mellor-Yamada
Turbulence closure
Validation

16. SECURITY CLASSIFICATION OF:			17. LIMITATION OF ABSTRACT	18. NUMBER OF PAGES	19a. NAME OF RESPONSIBLE PERSON
a. REPORT	b. ABSTRACT	c. THIS PAGE			Gaurav Savant
Unclassified	Unclassified	Unclassified	SAR	33	19b. TELEPHONE NUMBER *(Include area code)* 601-634-3213